Exact Solutions of Functionally Gradient Piezothermoelastic Cantilevers and Parameter Identification

CHEN YING AND SHI ZHIFEI*

School of Civil Engineering, Beijing Jiaotong University, Beijing, 100044, China

ABSTRACT: Based on the theory of elasticity, some exact solutions of functionally gradient piezothermoelastic cantilevers under different coupled loadings are obtained. As an application, these solutions have been successfully used to identify the gradient piezoelectric parameter and the thermal material coefficients. Besides, some numerical results have been carried out for the cantilever under two different kinds of loadings. It is found that the tip deflection of the cantilever agrees very well with the experimental and theoretical findings provided by other investigations. The present study also shows that the linear change of thermal material parameters does not influence the distribution of the stress and induction of the cantilever. But it influences the components of strain and electric field strength as well as the displacement and electric potential of the cantilever.

Key Words: FGM, piezothermoelastic material, sensors and actuators, inverse problem, parameter identification

INTRODUCTION

SINCE the Curie brothers found the piezoelectric effect in 1880, piezoelectric materials have found wide applications in engineering, and many important achievements have been obtained, such as the investigations on piezoelectric ultrasonic motors (Philippe and Kenji, 2003), vibration control of different kinds of structures (Clark, 2000; Corr and Clark, 2001; Vázquez and Kenji, 2001), actuators (Alexander and Brei, 2003; Sirohi and Chopra, 2000a, 2003; Vendlinski and Brei, 2003), and so on.

In engineering applications, piezoelectric materials are usually designed as unimorph with one layer or bimorph with two layers, which are mechanically jointed by a glue layer (Kenji, 1997; Kielczyński et al., 1998; Pritchard and Bowen, 2002; Hou and Chen, 2003). Sirohi and Chopra (2000b) gave a detailed discussion on strain measurements from piezoceramic (PZT) and piezo-film (PVDF) sensors and compared them with strains from a conventional foil strain gage. The principal weakness of these sandwich devices is that the bonding layer may crack at a low temperature and creep or peel off at a high temperature, which will reduce the lifetime and reliability of these piezoelectric devices. Sometimes, thermal loading is so far from being the predominant reason of failure of these smart structures. Hence, the effects of thermal loading have attracted a considerable amount of attention in recent years. For example, Schulz et al. (2003) discussed the general properties and modeling of piezoelectric materials at moderately elevated temperatures. Raja et al. (1999) presented a generalized piezothermoelastic finite element formulation of a laminated beam with embedded piezoelectric material as distributed actuators/sensors. Victor (1996) studied the effects of temperature on piezoelectric sensors and on a composite substrate, and found that even moderate fluctuations of temperature within 200°C can significantly change the voltage reading from a piezoelectric sensor. Tian and Shen (2003) finished a numerical analysis of thermomechanical behavior of piezoelectric structures under finite deformation.

To improve the durability of piezoelectric structures, functionally gradient piezoelectric materials (FGPM) were developed and have been used to produce devices, such as sensors and actuators (Zhu et al., 1995; Qiu et al., 2003). When piezoelectric materials are designed with gradient in one or two dimensions, they can overcome the peeling and cracking of the glue layer and at the same time reduce the mechanical stress. Based on a simple analytical model, Hauke et al. (2000) investigated a kind of multimorph piezoelectric actuator and predicted the behavior of functionally gradient material (FGM) actuators. Based on the theory of primary elasticity, Kruusing (2000) gave not only some solutions for cantilever with gradient

*Author to whom correspondence should be addressed.
E-mail: zfshi178@sohu.com

1045-389X/05/06 0531–9 $10.00/0 DOI: 10.1177/1045389X05053208

material properties but also a brief review of design and modeling for cantilever microactuators. Kouvatov et al. (1999) compared the bending behavior of bimorphic and polymorphic bending actuators based on finite element analysis. For the following three kinds of piezoelectric cantilevers: (A) there is a potential function for body forces (Shi, 2002), (B) the piezoelectric parameter g_{31} changes linearly (Liu and Shi, 2004) and (C) the elastic parameter S_{33} and body forces change simultaneously (Shi and Chen, 2004), the elastic analyses are provided and the fundamental solutions are obtained.

Despite a considerable number of works on smart materials and structures, only a few research papers are related to the perfectly gradient piezothermoelastic materials, especially those considering these materials under complicated loading cases. In this article, a functionally gradient piezothermoelastic cantilever subjected to different coupled loadings is studied based on the theory of elasticity. Some exact solutions are obtained and used to identify the gradient piezoelectric parameter (g_{31}) and the thermal material coefficient (q_3). As a special case, the tip deflection of the cantilever obtained in the present study is compared with that from both experimental and other analytical models based on $BaTiO_3$-ceramics, and a good agreement is found. At the end of this article, some inherent properties of the exact solutions are discussed.

BASIC EQUATIONS FOR PIEZOTHERMOELASTIC MATERIALS UNDER PLANE STRAIN CONDITION

The cantilever that is often used as the model for analyzing piezoelectric sensors and actuators (Kielczyński et al., 1998; Kruusing, 2000), shown in Figure 1, is studied. The upper and lower surfaces of the beam are continuously adhered to electrodes. To describe the basic equations of the problem clearly, the Cartesian coordinate system (x, z) is introduced in the present analysis. Let ε_{ij}, σ_{ij}, D_i, E_i denote the components of strain, stress, induction, and electric field strength of piezoelectric media, respectively. The constitutive equations for the piezothermoelastic material under plane strain condition can be obtained and expressed as (Zhong and Shang, 2003)

$$\begin{cases} \varepsilon_x = S_{11}\sigma_x + S_{13}\sigma_z + g_{31}D_z - \mu_{11}\theta \\ \varepsilon_z = S_{13}\sigma_x + S_{33}\sigma_z + g_{33}D_z - \mu_{33}\theta \\ \gamma_{xz} = S_{44}\tau_{xz} + g_{15}D_x \end{cases} \tag{1a}$$

$$\begin{cases} E_x = -g_{15}\tau_{xz} + \zeta_{11}D_x \\ E_z = -g_{31}\sigma_x - g_{33}\sigma_z + \zeta_{33}D_z - q_3\theta \end{cases} \tag{1b}$$

where S_{ij}, g_{ij}, and ζ_{ij} are the coefficients of the effective elastic compliance, piezoelectric and dielectric impermeability, respectively; θ is the temperature rise; μ_{ii} and q_3 are thermal strain and pyroelectric coefficients of the material, respectively. Without considering body force and body charge, the equilibrium equations can be written as:

$$\begin{cases} \dfrac{\partial \sigma_x}{\partial x} + \dfrac{\partial \tau_{xz}}{\partial z} = 0 \\ \dfrac{\partial \tau_{xz}}{\partial x} + \dfrac{\partial \sigma_z}{\partial z} = 0 \end{cases} \tag{2a}$$

$$\frac{\partial D_x}{\partial x} + \frac{\partial D_z}{\partial z} = 0 \tag{2b}$$

$$\frac{\partial}{\partial x}\left(k_{11}\frac{\partial \theta}{\partial x}\right) + \frac{\partial}{\partial z}\left(k_{33}\frac{\partial \theta}{\partial z}\right) = 0 \tag{2c}$$

where k_{ii} is the coefficient of thermal conductivity. The components of strain and electric field strength are related to the displacement (u, w) and electrical potential ϕ by the following equations:

$$\begin{cases} \varepsilon_x = \dfrac{\partial u}{\partial x}, \quad \varepsilon_z = \dfrac{\partial w}{\partial z}, \quad \gamma_{xz} = \dfrac{\partial u}{\partial z} + \dfrac{\partial w}{\partial x} \\ E_x = -\dfrac{\partial \phi}{\partial x}, \quad E_z = -\dfrac{\partial \phi}{\partial z} \end{cases} \tag{3}$$

It is realized that the piezoelectric parameter (g_{31}) plays an important role in the judgment on the behavior of piezoelectric materials and the performances of piezoelectric products. A lot of investigations (Marcus, 1984; Hauke et al., 2000; Kruusing, 2000) have been made on the properties of piezoelectric materials with different values of g_{31}. In the present analysis, we focus on the exact solutions of a piezothermoelastic cantilever. The gradient property of piezoelectric parameter (g_{31}) is taken into account, while without loss of generality, other material parameters are assumed to be constants. In detail, the gradient property of piezoelectric parameter (g_{31}) is assumed as:

$$g_{31} = r_1 z + r_2 \tag{4}$$

where r_1 and r_2 are the material constants. Equations (1)–(3) together with some suitable boundary conditions can be used to study a piezoelectric thermoelectroelastic boundary value problem. The substitution of Equations (1) and (2) into Equation (3) results in the

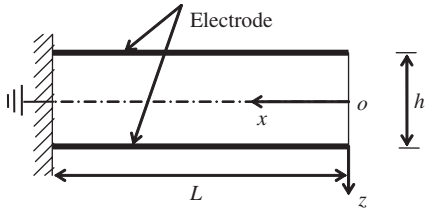

Figure 1. *Schematic of the piezoelectric cantilever.*

following governing equations in terms of the stress σ_x, σ_z and induction D_x, D_z:

$$\begin{cases} \left[S_{11}\dfrac{\partial^2}{\partial z^2}+\left(S_{13}+\dfrac{S_{44}}{2}\right)\dfrac{\partial^2}{\partial x^2}\right]\sigma_x \\ \quad+\left[S_{33}\dfrac{\partial^2}{\partial x^2}+\left(S_{13}+\dfrac{S_{44}}{2}\right)\dfrac{\partial^2}{\partial z^2}\right]\sigma_z \\ \quad+(r_1 z+r_2)\dfrac{\partial^2 D_z}{\partial z^2}+g_{33}\dfrac{\partial^2 D_z}{\partial x^2}+2r_1\dfrac{\partial D_z}{\partial z} \\ \quad-g_{15}\dfrac{\partial^2 D_x}{\partial x\partial z}-\mu_{11}\dfrac{\partial^2\theta}{\partial z^2}-\mu_{33}\dfrac{\partial^2\theta}{\partial x^2}=0 \\ (r_1 z+r_2+g_{15})\dfrac{\partial\sigma_x}{\partial x}+g_{33}\dfrac{\partial\sigma_z}{\partial x}+\zeta_{11}\dfrac{\partial D_x}{\partial z} \\ \quad-\zeta_{33}\dfrac{\partial D_z}{\partial x}+q_3\dfrac{\partial\theta}{\partial x}=0 \end{cases} \tag{5}$$

In fact, Equation (5) is the compatibility equation that makes it possible to find the displacement and electrical potential when the stress and induction are obtained.

EXACT SOLUTIONS OF A PIEZOTHERMOELASTIC CANTILEVER UNDER COUPLED LOADINGS

For the piezoelectric cantilever, shown in Figure 1, subjected to coupled thermal and mechanical/electric loadings, the exact solutions can be found based on the theory of elasticity. The temperature field can be easily obtained first.

Temperature Field

Assume that the piezoelectric cantilever is homogeneously heated at the upper surface and the temperature of the upper and lower surfaces of the beam is kept constant at θ_0 and 0, respectively. This means we have the following thermal boundary conditions:

$$\theta\left(x,\frac{h}{2}\right)=0,\quad \theta\left(x,-\frac{h}{2}\right)=\theta_0 \tag{6}$$

In this case, Equation (2c) becomes

$$k_{33}\frac{\partial^2\theta}{\partial z^2}=0 \tag{7}$$

So the temperature field of the cantilever can be easily obtained as:

$$\theta=A+Bz \tag{8}$$

where $A=\theta_0/2,\ B=-\theta_0/h$.

Mechanical and Electric Fields

Keeping Equation (8) in mind, the compatibility equation (5) can be rewritten as:

$$\begin{cases} \left[S_{11}\dfrac{\partial^2}{\partial z^2}+\left(S_{13}+\dfrac{S_{44}}{2}\right)\dfrac{\partial^2}{\partial x^2}\right]\sigma_x \\ \quad+\left[S_{33}\dfrac{\partial^2}{\partial x^2}+\left(S_{13}+\dfrac{S_{44}}{2}\right)\dfrac{\partial^2}{\partial z^2}\right]\sigma_z \\ \quad+(r_1 z+r_2)\dfrac{\partial^2 D_z}{\partial z^2}+g_{33}\dfrac{\partial^2 D_z}{\partial x^2} \\ \quad+2r_1\dfrac{\partial D_z}{\partial z}-g_{15}\dfrac{\partial^2 D_x}{\partial x\partial z}=0 \\ (r_1 z+r_2+g_{15})\dfrac{\partial\sigma_x}{\partial x}+g_{33}\dfrac{\partial\sigma_z}{\partial x} \\ \quad+\zeta_{11}\dfrac{\partial D_x}{\partial z}-\zeta_{33}\dfrac{\partial D_z}{\partial x}=0 \end{cases} \tag{9}$$

To find the mechanical and electrical fields of the piezoelectric cantilever, the Airy stress function method is used. The stress function φ and induction function ψ are introduced. The components of stress and induction can be expressed as:

$$\begin{cases} \sigma_x=\dfrac{\partial^2\varphi}{\partial z^2},\quad \sigma_z=\dfrac{\partial^2\varphi}{\partial x^2},\quad \tau_{xz}=-\dfrac{\partial^2\varphi}{\partial x\partial z} \\ D_x=\dfrac{\partial\psi}{\partial z},\quad D_z=-\dfrac{\partial\psi}{\partial x} \end{cases} \tag{10}$$

To find the solutions, the following two kinds of coupled loadings are considered separately.

Case I: Cantilever Subjected to Thermal and Electric Loadings

Besides being subjected to thermal loading, the piezoelectric cantilever is also subjected to an electric loading, as shown in Figure 2. That is to say, there is an electric potential difference between the upper and lower surfaces of the cantilever

$$\phi\left(x,-\frac{h}{2}\right)-\phi\left(x,\frac{h}{2}\right)=V_0 \tag{11}$$

In this case, the stress function and induction function can be assumed as:

$$\varphi=0\quad\text{and}\quad\psi=bx \tag{12}$$

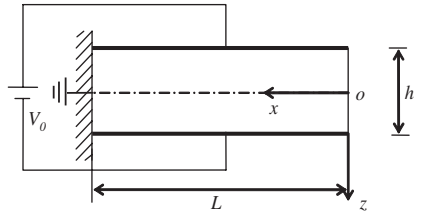

Figure 2. *The cantilever subjected to thermal loading and electric field.*

where b is an unknown constant to be determined later. Substituting Equation (12) into Equation (10), the expressions of stress and induction can be obtained as:

$$\sigma_x = \sigma_z = \tau_{xz} = D_x = 0 \quad \text{and} \quad D_z = -b \tag{13}$$

It is obvious that the compatibility equation (9) is automatically satisfied in this case. Besides, the stress and induction also satisfy all the following boundary conditions, i.e.,

Mechanical boundary conditions

$$\begin{cases} \tau_{xz} = \sigma_z = 0 & \text{at } z = \pm h/2 \\ \tau_{xz} = \sigma_x = 0 & \text{at } x = 0 \end{cases} \tag{14a}$$

Electric boundary conditions

$$D_x = 0 \quad \text{at } x = 0, L \tag{14b}$$

Using Equation (1), the strain components and electric field strength can be obtained as:

$$\begin{cases} \varepsilon_x = -(r_1 z + r_2)b - \mu_{11}(A + Bz) \\ \varepsilon_z = -g_{33}b - \mu_{33}(A + Bz) \\ \gamma_{xz} = 0 \end{cases} \tag{15a}$$

$$\begin{cases} E_x = 0 \\ E_z = -\varsigma_{33}b - q_3(A + Bz) \end{cases} \tag{15b}$$

To determine the displacement and the electric potential of the cantilever, the following boundary conditions are considered:

$$u(L,0) = 0, \quad w(L,0) = 0, \quad \frac{\partial w(L,0)}{\partial x} = 0 \quad \text{and} \quad \phi(L,0) = 0 \tag{16}$$

By integrating Equation (3), and using the above boundary conditions and Equation (11), the displacement components and electric potential as well as the unknown constant b can be determined as:

$$\begin{cases} u = (r_1 z + r_2)b(L - x) + \mu_{11}(A + Bz)(L - x) \\ w = -g_{33}bz - \mu_{33}\left(Az + \dfrac{B}{2}z^2\right) \\ \qquad + \dfrac{1}{2}(r_1 b + B\mu_{11})(x^2 - 2xL + L^2) \end{cases} \tag{17a}$$

$$\phi = \varsigma_{33}bz + q_3\left(Az + \frac{B}{2}z^2\right) \tag{17b}$$

where

$$b = -\frac{q_3 Ah + V_0}{\varsigma_{33}h} \tag{18}$$

The above analysis and solutions show that the coupled thermal and electric loadings do not lead to stress components in the perfectly gradient piezoelectric cantilever. This conclusion demonstrates that the predication (Hauke et al., 2000) is correct. For the distribution of electric potential on any cross section of the beam, a quadratic expression is found.

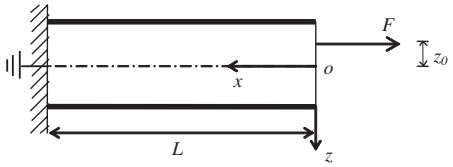

Figure 3. *The cantilever subjected to thermal loading and eccentric load.*

Case II: Cantilever Subjected to Thermal and Mechanical Loadings

For the piezoelectric cantilever shown in Figure 3, besides being subjected to thermal loading, an eccentric load F is also applied at the free end. In this case, the stress function and induction function can be assumed as:

$$\varphi = -az^3 - cz^2 \quad \text{and} \quad \psi = 0 \tag{19}$$

where a and c are unknown constants to be determined. Then the components of stress and induction can be obtained using Equation (10) as:

$$\sigma_x = -6az - 2c, \quad \sigma_z = \tau_{xz} = D_x = D_z = 0 \tag{20}$$

It is obvious that the compatibility equation (9) is satisfied. Besides, some of the mechanical and electric boundary conditions are also automatically satisfied, i.e.,

$$\begin{cases} \tau_{xz} = \sigma_z = D_z = 0 & \text{at } z = \pm h/2 \\ D_x = 0 & \text{at } x = 0, L \end{cases} \tag{21}$$

To satisfy the mechanical boundary conditions at the free end of the cantilever, Saint-Venant's principle is introduced, i.e.,

$$\begin{aligned} &\tau_{xz} = 0, \quad \int_{-h/2}^{h/2} \sigma_x \, \mathrm{d}z = F, \\ &\int_{-h/2}^{h/2} \sigma_x z \, \mathrm{d}z = -Fz_0 \qquad \text{at} \quad x = 0 \end{aligned} \tag{22}$$

Substituting Equation (20) into Equation (22), we get

$$a = \frac{2Fz_0}{h^3}, \quad c = -\frac{F}{2h} \tag{23}$$

Using Equation (1), the strain components and electric field strength can be obtained as:

$$\begin{cases} \varepsilon_x = -2S_{11}c - \mu_{11}A - (6S_{11}a + B\mu_{11})z \\ \varepsilon_z = -2S_{13}c - \mu_{33}A - (6S_{13}a + B\mu_{33})z \\ \gamma_{xz} = 0_x \end{cases} \tag{24a}$$

$$\begin{cases} E_x = 0 \\ E_z = 6ar_1z^2 + (2cr_1 + 6ar_2 - q_3B)z + 2cr_2 - q_3A \end{cases} \tag{24b}$$

Furthermore, the displacement and electric potential can be obtained respectively as follows:

$$\begin{cases} u = (2S_{11}c + A\mu_{11})(L - x) + (6S_{11}a + B\mu_{11})(L - x)z \\ w = -\dfrac{1}{2}(6S_{13}a + B\mu_{33})z^2 - (2S_{13}c + \mu_{33}A)z \\ \qquad + \dfrac{1}{2}(6S_{11}a + B\mu_{11})(x^2 - 2Lx + L^2) \end{cases} \tag{25a}$$

$$\phi = -2ar_1z^3 - \frac{1}{2}(2cr_1 + 6ar_2 - Bq_3)z^2 - (2cr_2 - Aq_3)z \tag{25b}$$

It can be found from this solution that all the stress components except σ_x are zero when the cantilever is subjected to an eccentric load F and a thermal loading. The cubic expression for the distribution of electric potential on any cross section of the cantilever is also derived.

PARAMETER IDENTIFICATION

As a kind of inverse problem, parameter identification plays an important role in precisely describing the internal behavior of a FGM. For a gradient material, it is very difficult, or impossible to process a homogeneous specimen to measure the properties of a concerned material point by using a general method (Bui, 1993). Much attention has been given as to how to identify a non-homogeneous material. As an inverse problem, Ashida and Tauchert (1997) determined the temperature field of a contacting body using a potential function approach including three displacement potentials and two electric potentials. Liu et al. (2001) presented a computational inverse procedure for the characterization of material properties of FGMs using the surface displacement response of the plate. Franke et al. (2002) measured the temperature dependencies of the real and imaginary parts of the coefficient s_{11}^E by using the method of piezoelectric resonance. Fang (1999) developed a simple technique to characterize the elastic moduli of thin films of any thickness. In the present article, the method to identify the material parameters for functionally gradient piezothermoelastic materials is discussed.

Identification of Piezoelectric Parameter (g_{31})

Based on the results obtained in the above sections, the piezoelectric parameter (g_{31}) can be identified. To determine the unknown parameters (r_1 and r_2) in Equation (4), a cantilever loaded axially by a concentrated force F at the free end, as shown in Figure 4, is considered. Ignoring the temperature rise of the beam, the electric potential of the beam can be obtained from Equation (25b) as:

$$\phi = \frac{F}{2h}r_1z^2 + \frac{F}{h}r_2z \tag{26}$$

Let ϕ_U and ϕ_L denote the electric potential at the upper and lower surfaces of the beam, respectively. Then the parameters (r_1 and r_2) can be found as:

$$r_1 = \frac{4(\phi_U + \phi_L)}{Fh}, \quad r_2 = \frac{\phi_L - \phi_U}{F} \tag{27}$$

The above formulas demonstrate that once the electric potential at the upper and lower surfaces of the cantilever is obtained from the tests, the piezoelectric parameter (g_{31}) can be identified.

Identification of Pyroelectric Coefficient (q_3)

For the case when the cantilever is loaded by a temperature rise and a concentrated force simultaneously, as shown in Figure 4, the electric potential of the cantilever can be deduced from Equation (25b) as follows:

$$\phi = \left(\frac{B}{2}z^2 + Az\right)q_3 - (r_1z^2 + 2r_2z)c \tag{28}$$

Further, if the symbol ϕ_{LFT} is used to denote the electric potential at the lower surface of the beam under this coupled thermal and mechanical loadings, the pyroelectric coefficient (q_3) can be identified as:

$$q_3 = \frac{8\phi_{LFT} + (2r_1h^2 + 8r_2h)c}{(h^2B + 4hA)} = \frac{8\phi_{LFT} + (2r_1h^2 + 8r_2h)c}{h\theta_0} \tag{29}$$

If the cantilever is loaded by a thermal loading only, then we have

$$q_3 = \frac{8\phi_{LT}}{h\theta_0} \tag{30}$$

where the symbol ϕ_{LT} denotes the electric potential detected at the lower surface of the cantilever in this loading case. Equation (30) shows that once the electric

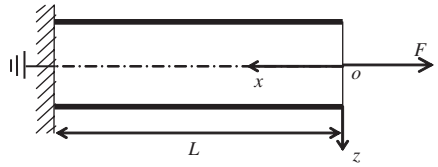

Figure 4. *The cantilever subjected to concentrated load.*

potential at the lower surface is detected when a temperature rise is provided at the upper surface of the cantilever only, the pyroelectric coefficient (q_3) can be identified.

SPECIAL LOADING CASES AND COMPARISONS

Besides being used to identify material parameters, the results obtained in the above sections can also be used to some special loading cases and lead to some simple results. In this section, two special loading cases are discussed. The geometric parameters of the cantilever discussed in the investigation by Hauke et al. (2000) are adopted, i.e., $L = 16\,\text{mm}$ and $h = 1.32\,\text{mm}$. Some changes in physical quantities of the cantilever under thermal loading are obtained. Besides, some results given in the present article under electric loading are compared with those obtained in the experimental and theoretical investigations (Hauke et al., 2000) and a good agreement is found.

Cantilever Subjected to Thermal Loading Only

If the cantilever is subjected to a temperature rise only, the solutions can be directly deduced from the findings obtained in Case I by assuming $V_0 = 0$ and $\varsigma_{33} \to \infty$ or in Case II by assuming $F = 0$. In detail, we can obtain the following simple expressions:

Stress and induction components

$$\sigma_x = \sigma_z = \tau_{xz} = D_x = D_z = 0 \tag{31}$$

Strain and electric field strength components

$$\begin{cases} \varepsilon_x = -\mu_{11}(A + Bz), \quad \varepsilon_z = -\mu_{33}(A + Bz), \quad \gamma_{xz} = 0 \\ E_z = -q_3(A + Bz), \quad E_x = 0 \end{cases} \tag{32}$$

Displacement components and electric potential

$$\begin{cases} u = \mu_{11}\left(\dfrac{1}{2} - \dfrac{z}{h}\right)(L - x)\theta_0 \\ w = -\dfrac{\mu_{33}}{2}\left(z - \dfrac{z^2}{h}\right)\theta_0 - \dfrac{\mu_{33}}{2h}(x^2 - 2Lx + L^2)\theta_0 \\ \phi = \dfrac{q_3}{2}\left(z - \dfrac{z^2}{h}\right)\theta_0 \end{cases} \tag{33}$$

For the cantilever made of cadmium selenide and polarized in the thickness direction, the following material parameters $\mu_{11} = -2.16 \times 10^{-6}\,1/\text{K}$, $\mu_{33} = -1.76 \times 10^{-6}\,1/\text{K}$, and $q_3 = -2.95 \times 10^4\,\text{N}/(\text{K C})$ are used in the present study (Kapuria et al., 1996). The longitudinal and transverse displacements of every point at the upper surface of the actuator are plotted in Figures 5 and 6, respectively, for the different temperature rises 1, 2, and 5 K. Figure 7 shows the distribution of electric potential at any cross section of the beam under different temperature rises. These results are consistent with the findings obtained by Kapuria et al. for a finite

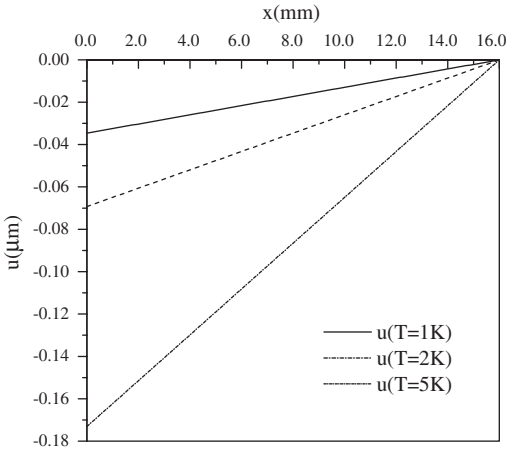

Figure 5. *The longitudinal displacement u at z = −h/2.*

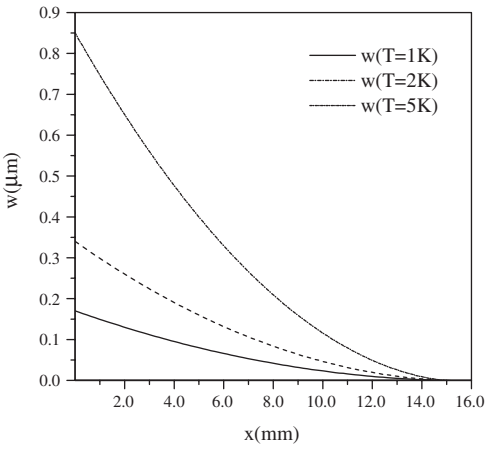

Figure 6. *The transverse displacement w at z = −h/2.*

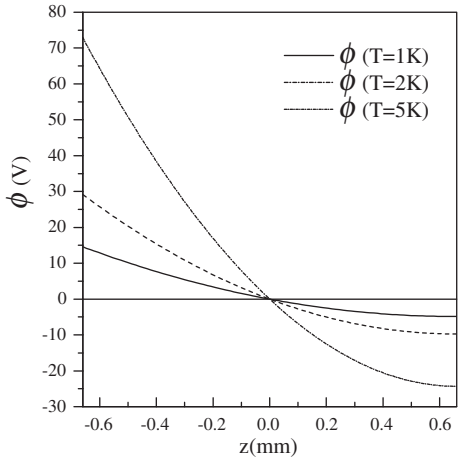

Figure 7. *The electric potential distribution at any cross section of the cantilever.*

transversely isotropic piezothermoelastic axisymmetric cylindrical shell.

Cantilever Subjected to Electric Field Only

If the cantilever is subjected to an electric field only, the solutions can be directly deduced from the findings obtained in Case I by assuming $\theta_0 = 0$ as:

Stress and induction components

$$\sigma_x = \sigma_z = \tau_{xz} = D_x = 0, \quad D_z = \frac{V_0}{h\varsigma_{33}} \tag{34}$$

Strain and electric field strength components:

$$\begin{cases} \varepsilon_x = \dfrac{V_0}{\varsigma_{33}h}(r_1 z + r_2), \quad \varepsilon_z = \dfrac{V_0 g_{33}}{\varsigma_{33}h}, \quad \gamma_{xz} = 0 \\ E_z = \dfrac{V_0}{h}, \quad E_x = 0 \end{cases} \tag{35}$$

Displacement components and electric potential

$$\begin{cases} u = -\dfrac{V_0}{\varsigma_{33}h}(r_1 z + r_2)(L - x) \\ w = \dfrac{V_0}{\varsigma_{33}h}\left[g_{33}z - \dfrac{1}{2}r_1(x^2 - 2xL + L^2)\right] \\ \phi = -\dfrac{V_0}{h}z \end{cases} \tag{36}$$

Now let us compare the results obtained in the present study with some experimental and theoretical findings obtained in another investigation (Hauke et al., 2000). To do so, the transverse deflection of the cantilever caused only by an electric voltage loading is rewritten as follows:

$$w = \frac{V_0}{\varsigma_{33}h}\left[g_{33}z - \frac{1}{2}r_1(x^2 - 2xL + L^2)\right] \tag{37}$$

Based on the elementary theory of elasticity and following the procedure introduced by Marcus (1984), Hauke et al. (2000) obtained the tip deflection (δ) at the free end of the actuator as:

$$\delta(N) = \frac{E_3 L^2 d_{31}^{\max}}{h}\left(\frac{N+1}{N}\right) \tag{38}$$

where E_3 is the applied electric field, $d_{31}^{\max}$ is the piezoelectric parameter of the lower layer of the beam. In Hauke et al.'s investigation on $BaTiO_3$-ceramics bending actuators, the FGM specimens consisted of N layers with different piezoelectric properties. For simplicity, the dielectric ($\varepsilon_{33}^T = 2000\,\mathrm{F/m}$) and other material parameters were assumed to be constant for all layers. Besides, each layer has the same thickness, given by the formula $t_L = h/N$ with $h = 1.32\,\mathrm{mm}$ and a surface area of $16 \times 4\,\mathrm{mm}^2$.

Based on the relations of piezoelectric parameters, all the material parameters used in the present study including the distribution of gradient parameter (g_{31}) can be determined for $BaTiO_3$-ceramics (Hauke et al., 2000). We have $g_{31} = 45.5z\,\mathrm{V\,pm/N}$ ($-h/2 \le z \le h/2$), $g_{33} = 0.08\,\mathrm{V\,pm/N}$, and $\varsigma_{33} = 0.0005\,\mathrm{m/F}$. According to Equation (37), the tip deflection $\delta = w(0, -h/2)$ related to the applied voltage is shown in Figure 8. The figure gives a slope of $m = \partial w/\partial V = 0.0089\,\mu\mathrm{m/V}$. For comparison, the linear regression of Hauke et al.'s experimental data for the trimorph actuator is also plotted in the same figure. Hauke et al.'s regression gives a slope of $m = 0.011\,\mu\mathrm{m/V}$.

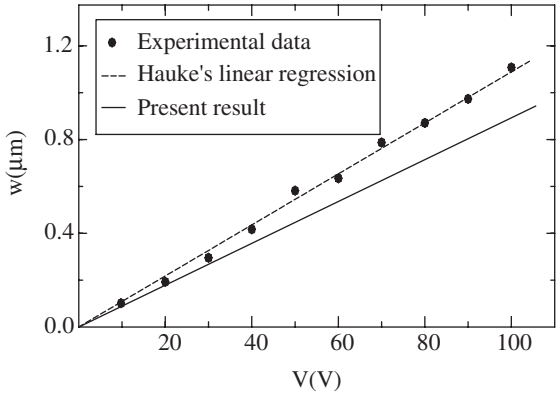

Figure 8. *Dependence of the tip deflection on the applied voltage.*

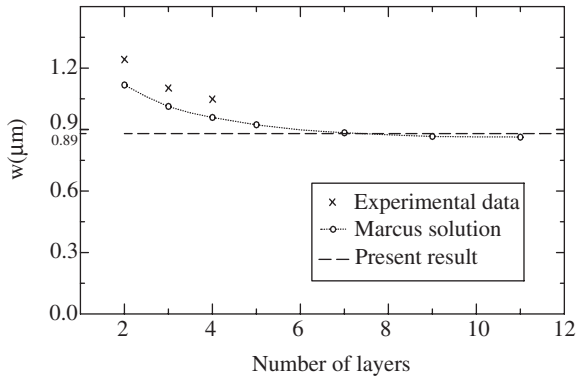

Figure 9. *Tip deflection of the actuator based on different analytical models at $V = 100\,V$.*

Figure 9 shows the relationship between the tip deflection and the number of layers of the actuator at $V = 100\,\mathrm{V}$ (corresponding to an effective field of $0.75\,\mathrm{kV/cm}$) according to Marcus' analytical model and experimental results. According to Equation (37), the tip deflection determined by the present study is $0.89\,\mu\mathrm{m}$, which is also plotted in Figure 9. It can be seen that the tip deflections obtained by the experiment and by the N-morph analytical model decrease with increasing number of layers, and the tip deflection obtained in the present study is slightly smaller than that given by another investigation based on the N-morph model (Hauke et al., 2000). It is clear that the more the number of layers, the more the tip deflection inclining to the

result given in Equation (37), of the present article for FGM actuators.

DISCUSSION AND CONCLUSIONS

(1) In the analysis described above, all the thermal material coefficients are assumed to be constant. In this section, the thermal material coefficients with gradient properties are discussed. The thermal material parameters (μ_{11}, μ_{33}, and q_3) are assumed as changing linearly along the z-direction, which is sufficient for most engineering applications, i.e.,

$$\mu_{11} = m_1 z + m_2, \quad \mu_{33} = n_1 z + n_2, \quad q_3 = t_1 z + t_2 \quad (39)$$

Combining Equations (1), (4), and (39), the compatibility equation can be rewritten as:

$$\begin{cases} \left[S_{11}\dfrac{\partial^2}{\partial z^2} + \left(S_{13} + \dfrac{S_{44}}{2}\right)\dfrac{\partial^2}{\partial x^2}\right]\sigma_x \\ \quad + \left[S_{33}\dfrac{\partial^2}{\partial x^2} + \left(S_{13} + \dfrac{S_{44}}{2}\right)\dfrac{\partial^2}{\partial z^2}\right]\sigma_z \\ \quad + (r_1 z + r_2)\dfrac{\partial^2 D_z}{\partial z^2} + g_{33}\dfrac{\partial^2 D_z}{\partial x^2} + 2r_1\dfrac{\partial D_z}{\partial z} - g_{15}\dfrac{\partial^2 D_x}{\partial x \partial z} \\ \quad - (m_1 z + m_2)\dfrac{\partial^2 \theta}{\partial z^2} - (n_1 z + n_2)\dfrac{\partial^2 \theta}{\partial x^2} = 0 \\ (r_1 z + r_2 + g_{15})\dfrac{\partial \sigma_x}{\partial x} + g_{33}\dfrac{\partial \sigma_z}{\partial x} + \zeta_{11}\dfrac{\partial D_x}{\partial z} \\ \quad - \zeta_{33}\dfrac{\partial D_z}{\partial x} + (t_1 z + t_2)\dfrac{\partial \theta}{\partial x} = 0 \end{cases} \quad (40)$$

It is obvious that the components of stress and induction as well as the temperature field obtained in the present study for every considered loading case satisfy Equation (40). In other words, the linear change of thermal material parameters (μ_{11}, μ_{33}, and q_3) does not influence the distribution of the stress and induction for the cantilever. But it tremendously influences the distribution of strain, electric field strength, and the components of displacements as well as the electric potential of the cantilever.

(2) Based on the theory of elasticity, the present analysis provides some exact solutions for functionally gradient piezothermoelastic cantilevers under some coupled loading cases.

(3) As a kind of inverse problem, the solutions obtained in the present study have been successfully used to determine the gradient profile for piezoelectric parameter (g_{31}). In the present analysis, the piezoelectric parameter (g_{31}) and the thermal material coefficient (q_3) are identified based on the results of the cantilever under an electric loading. It is easily understood that the parameters can also be identified in terms of the displacement components of the cantilever.

(4) The longitudinal displacement u changes linearly with the coordinate x under both electric loading and temperature rise. The plane of any cross section before loading remains in plane after loading for the above two loading cases. The transverse displacement w caused by electric loading or temperature rise is quadratic with the coordinate x. The electric potential changes linearly with z at any cross section when an electric loading is applied but the distribution will be quadratic when the temperature rise is provided.

(5) The tip deflection of the actuator with gradient behavior is slightly smaller than that of the N-morph model. The more the number of layers of the N-morph model, the more the tip deflection inclining to the result given in the present article for FGM actuators.

ACKNOWLEDGMENTS

This work is supported by the National Natural Science Foundation of China (50272003) and by the Teaching and Research Award Fund for Outstanding Young Teachers in Higher Education Institutions of MOE PRC.

REFERENCES

Alexander, Paul W. and Brei, Diann 2003. "Piezoceramic Telescopic Actuator Quasi-static Experimental Characterization," *Journal of Intelligent Materials Systems and Structures*, 14(10):643–656.

Ashida, Fumihiro and Tauchert, Theodore R. 1997. "Temperature Determination for a Contacting Body based on an Inverse Piezothermoelastic Problem," *International Journal of Solids and Structures*, 34(20):2549–2561.

Bui, H.D. 1993. *Introduction Aux Problems Inverses en Mecanique des Materiaux*, Direction des Etudes et Recherches d′ Electricité de France/Editions EYROLLES, Paris.

Clark, William W. 2000. "Vibration Control with State-switched Piezoelectric Materials," *Journal of Intelligent Material Systems and Structures*, 11(4):263–271.

Corr, L.R. and Clark, W.W. 2001. *Energy Dissipation Analysis of Piezoceramic Semi-active Vibration Control, Structures, Structural Dynamics, and Materials Conference*, Seattle, WA, April 16–19.

Franke, Iwona, Roleder, Krystian, Miga, Seweryn, Maillard, Alain and Kugel, Godefroy 2002. "Determination of the Elastic Properties of a $Li_2B_4O_7$ Single Crystal from the Piezoelectric Resonance," *Ferroelectrics*, 273:285–290.

Hauke, T., Kouvatov, A., Steinhausen, R., Seifert, W., Beige, H., Langhammer, H.T. and Abicht, H.P. 2000. "Bending Behavior of Functionally Gradient Materials," *Ferroelectrics*, 238:195–202.

Hou, Max Ti-Kuang and Chen, Rongshun 2003. "Effect of Width on the Stress-induced Bending of Micromachined Bilayer Cantilevers," *J. Micromech. Microeng.*, 13(1):141–148.

Kapuria, S., Dumir, P.C. and Sengupta, S. 1996. "Exact Piezothermoelastic Axisymmetric Solution of a Finite Transversely Isotropic Cylindrical Shell," *Comput. Struct.*, 61(6):1085–1099.

Kielczyński, P., Pajewski, W. and Szalewski, M. 1998. "Piezoelectric Sensors for Investigations of Microstructures," *Sensors and Actuators*, A65(1):13–18.

Kouvatov, A., Steinhausen, R., Seifert, W., Hauke, T., Langhammer, H.T., Beige, H. and Abicht, H. 1999. "Comparison between Bimorphic and Polymorphic Bending Devices," *Journal of the European Ceramic Society*, 19(6–7):1153–1156.

Kruusing, A. 2000. "Analysis and Optimization of Loaded Cantilever Beam Microactuators," *Smart Materials and Structures*, 9(2):186–196.

Liu, T.T. and Shi, Z.F. 2004. "Bending Behavior of Functionally Gradient Piezoelectric Cantilever," *Ferroelectrics*, 308:43–51.

Liu, G.R., Han, X. and Lam, K.Y. 2001. "Material Characterization of FGM Plates using Elastic Waves and an Inverse Procedure," *Journal of Composite Materials*, 35(11):954–971.

Marcus, M.A. 1984. "Performance Characteristics of Piezoelectric Polymer Flexure Mode Devices," *Ferroelectrics*, 57:203–220.

Philippe, Bouchilloux and Kenji, Uchino 2003. "Combined Finite Element Analysis – Genetic Algorithm Method for the Design of Ultrasonic Motors," *Journal of Intelligent Materials Systems and Structures*, 14(10):657–667.

Pritchard, Jane and Bowen, Chris Rhys 2002. "Characterization of Mulyi-layer Actuators," *Ferroelectrics*, 273:255–260.

Qiu, Jinhao, Tani, Junji, Ueno, Toshiyuki, Morita, Teppei, Takahashi, Hirofumi and Du, Hejun 2003. "Fabrication and High Durability of Functionally Gradient Piezoelectric Bending Actuators," *Smart Materials and Structures*, 12(1):115–121.

Raja, S., Rohwer, K. and Rose, M. 1999. "Piezothermoelastic Modeling and Active Vibration Control of Laminated Composite Beams," *Journal of Intelligent Material Systems and Structures*, 10(11):890–899.

Schult, Mark J., Sundaresan, Mannur, J., Mcmichael, Jason, Clayton, David, Sadler, Robert and Nagel, Bill. 2003. "Piezoelectric Materials at Elevated Temperature," *Journal of Intelligent Materials Systems and Structures*, 14(11):693–705.

Shi, Z.F. 2002. "General Solution of a Density Functionally Gradient Piezoelectric Cantilever and its Applications," *Smart Materials and Structures*, 11(1):122–129.

Shi, Z.F. and Chen, Y. 2004. "Functionally Graded Piezoelectric Cantilever Beam Under Load." *Archive of Applied Mechanics*, 74(3–4):237–247.

Sirohi, Jayant and Chopra, Inderjit 2000a. "Fundamental Behavior of Piezoceramic Sheet Actuators," *Journal of Intelligent Material Systems and Structures*, 11(1):47–61.

Sirohi, Jayant and Chopra, Inderjit 2000b. "Fundamental Understanding of Piezoelectric Strain Sensors," *Journal of Intelligent Material Systems and Structures*, 11(4):246–257.

Sirohi, Jayant and Chopra, Inderjit 2003. "Design and Development of a High Pumping Frequency Piezoelectric-hydraulic Hybrid Actuator," *Journal of Intelligent Materials Systems and Structures*, 14(3):135–147.

Tian, X.G. and Shen, Y.P. 2003. "Finite Element Analysis of Thermo-mechanical Behaviour of Piezoelectric Structures under Finite Deformation," *Acta mechanica solida sinica*, 24(2):169–178.

Uchino, Kenji 1997. *Piezoelectric Actuators and Ultrasonic Motors*, Kluwer Academic Publ., Boston/Dordrecht/London.

Vázquez, Carazo Alfredo and Kenji, Uchino 2001. "Novel Piezoelectric-based Power Supply for Driving Piezoelectric Actuators Designed for Active Vibration Damping Applications," *Journal of Electroceramics*, 7(3):197–210.

Vendlinski, James and Brei, Diann 2003. "Dynamic Behavior of Telescopic Actuators," *Journal of Intelligent Materials Systems and Structures*, 14(9):577–586.

Victor, Birman 1996. "Thermal Effects on Measurements of Dynamic Processes in Composite Structures using Piezoelectric Sensors," *Smart Materials and Structures*, 5(4):379–385.

Weileun, Fang 1999. "Determination of the Elastic Modulus of Thin Film Materials Using Self-deformed Micromachined Cantilevers," *J. Micromech. Microeng.*, 9(3):230–235.

Zhong, Z. and Shang, E.T. 2003. "Three Dimensional Exact Analysis of Functionally Gradient Piezothermoelectric Material Rectangular Plate," *Acta mechanical sinica*, 35(5): 542–552.

Zhu, X.H., Wang, Q. and Meng, Z.Y. 1995. "A Functionally Gradient Piezoelectric Actuator Prepared by Powder Metallurgical Process in PNN-PZ-PT System," *Journal of Materials Science Letters*, 14(7):516–518.